ISSN 0252-1075
Research Report No. RR-079

Contributions from
Indian Institute of Tropical Meteorology

DIAGNOSTIC MODEL OF THE SURFACE BOUNDARY LAYER - A NEW APPROACH

by

S. SINHA

PUNE - 411 008
INDIA

FEBRUARY 1999

CONTENTS

Diagnostic Model of the Surface Boundary Layer — A New Approach

By

Subroto Sinha

[Indian Institute of Tropical Meteorology, Pune – 411008, India]

Abstract

The diagnostic model of the Surface Layer (SL),described here, attempts to evaluate all the basic parameters, except those of moisture and moisture related parameters, using the wind and temperature observations at two levels only. It uses the Businger-type formulation of the non-dimensional profile functions for heat and momentum, but evaluates the "constants" used in these formulations, separately for each data set. The methodology of evaluating these constants is discussed in detail. The roughness heights for momentum and temperature are also evaluated separately for each data set. The Monin-Obukhov(M-O) stability length is obtained directly as a solution of a cubic equation, for unstable stratification, and as a solution of a quadratic equation, for stable stratification. The *Kansas Field Experiment Data* (1968), is used for computing the M-O stability lengths and the surface fluxes of heat and momentum. The computed values are in close agreement with the observed values of these parameters. Wind and temperature at all the standard levels were computed from the profile functions and compared with the corresponding observed values. The percentage differences between the two values are found to be very small.

The percentage differences are also evaluated using the iterative method with Businger's profile functions and a constant surface roughness height for momentum as well as for temperature. Both the roughness heights are taken to be the same. The percentage differences in this case were found to be much larger. A variable roughness height for momentum, as well as for temperature, reduced the percentage differences considerably. A method of computing the height of the surface boundary layer, has been developed and it is shown that the mean percentage differences between the computed and observed values of wind and temperature, are larger for those data levels which are above the surface layer.

List of symbols

C_p : Specific heat of air in SL, under constant pressure

f : Factor representing the ratio of "q" to "p" in the cubic equation of the SL

f_O Value of " f " in neutral stability

f_c : Coriolis parameter at the earth's surface

g : Acceleration due to gravity

h : Depth of the SL obtained by iteration

h_1 : Depth of the SL obtained by using empirical expression

H : Sensible heat flux at the surface

k : Von-Karman constant

K_m : Coefficient of eddy viscosity

L : Monin-Obukhov stability length

Ri : Gradient Richardson number

Ri_d : Richardson number at displacement height

T_i : Temperature at level " i "

T_s : Surface temperature

T_m : Mean representative absolute temperature of the SL

T_* : Turbulent temperature scale

TPr : Turbulent Prandtl number

u_* : Turbulent velocity scale or friction velocity

U_i : Total wind speed at level " i "

z : Vertical coordinate representing height above surface

Z_d Displacement height

z_o : Roughness height for momentum

z_{ot} : Roughness height for temperature

z_m : Geometric mean of the heights of the two lowest levels of observations

ρ : Density of dry air in SL

ξ : Non-dimensional height (= Z/L)

ξ_0 : Value of ξ at $Z=z_0$

ϕ_m : Non-dimensional profile function for wind

ϕ_h : Non-dimensional profile function for temperature

τ : Reynold's stress

τ_0 : Surface stress ($= \rho u_*^2$)

γ_1 : "Constant" used in the empirical profile function for wind in unstable stratification

γ_2 , γ_4 : "Constants" used in the empirical profile function for temperature in unstable stratification

γ_3 "Constant" used in the empirical profile function for wind and temperature in stable stratification

γ_5 : "Constant" used in the empirical profile function for temperature in stable stratification

α : Ratio of ϕ_m to ϕ_h

$[s' w']$: Vertical flux of the turbulent parameter s

1. Introduction

There is a growing realization amongst numerical modellers that the surface fluxes of momentum, heat and moisture, determine to a large extent the steady state of the atmosphere. Besides, the surface fluxes also determine the mean profiles of the parameters in the SL and in the atmospheric boundary layer. Direct measurement of these turbulent fluxes is difficult and expensive. A practical way is to devise a method of computing the fluxes accurately from a minimum number of observations, taken with the help of comparatively simpler instruments.

The most popular method of computing fluxes is the profile method, based on the similarity theory of Monin and Obukhov (1954). In this method flux-profile relationships are formulated, which express the vertical gradients of mean wind and temperature in terms of universal functions of a stability parameter. The form of these functions for various stabilty ranges is determined empirically from the data obtained from field experiments. The most widely used form of the functions are the ones obtained by Businger et al (1971), in which, certain universal constants are used. However, the similarity concept is based on an idealized model of the steady and plane parallel flow along a flat and homogeneous wall. The values of the universal functions computed from observed data show considerable scatter due to the deviations of the actual flow from the stated ideal conditions. A major contribution to these deviations appears to stem from conceptual deficiencies in defining the form of the universal functions in terms of certain "constants" and, in treating the roughness height, z_o, as a local parameter which is based only on the physical dimensions of the surface irregularities and therefore, constant for a particular location. In the earlier studies, there was no attempt to distinguish the roughness heights for momentum, z_o, and temperature, z_{ot}.

Berkowicz and Prahm (1982), gave a detailed evaluation of the profile method for estimation of sensible heat flux and friction velocity from wind and temperature data at two levels only, using numerical iteration. They showed that the error in estimating the friction velocity will be less, if an accurate value of z_o is used, as compared to using wind differences. According to Beljaars and Holstag (1991), the roughness height concept is only applicable to homogeneous terrain, whereas in practice, the terrain is very often inhomogeneous at all scales. Lo (1977), introduced a method based on the principle of weighted residuals, to evaluate the roughness height and the displacement height. The result of this study indicated that the roughness height is a function of the wind speed. An increase in the wind speed breaks up larger eddies into smaller ones at the top of the roughness elements, which increases the drag coefficient and roughness height. The roughness height for temperature is different from that for momentum, owing to the difference in transport mechanisms for heat and momentum, very close to the surface. In this model the values of z_o and z_{ot} are evaluated separately for each data set

Byun (1990), obtained analytical solutions of the surface layer equations using the profile functions in the form suggested by Businger et al (1971). In the case of unstable stratification, a cubic equation in the non-dimensional stability parameter, $\xi=Z/L$, is formed whose exact solution in terms of the gradient Richardson number is obtained. However, real solutions can be obtained only if certain conditions are

The present model attempts to adapt the Businger's form of the profile functions to the non-ideal nature of the flow, by computing the "constants" in the expression for the functions, for each data set, using certain formulations. The data obtained in the *Kansas Field Experiment* (1968), and published by Izumi et al (1971), are used in this study. The wind and temperature data at heights of 2m and 4m, respectively, are used to compute the following parameters of the SL:-

(a) The displacement height Z_d
(b) The Monin-Obukhov stability length, L, which is obtained analytically as a solution of certain algebraic equations.
(c) The turbulent velocity and temperature scales, u_* and T_* ,respectively.
(d) The roughness heights for momentum and temperature.
(e) The surface heat flux, H, and the surface temperature, T_s
(f) The depth of the SL and the coefficient of eddy viscosity, K_m, within the layer

2. Computation of SL Parameters

(a) *Displacement Height*

The displacement height Z_d expresses the adjustment of the representative height of measurement at the site of the observation, to account for possible upwind variations in relative terrain. It may depend on wind direction, the nature of the surface and stability. Some authors identify it as the height at which the extrapolated logarithmic wind profile intersects the Z-axis. It is treated as a constant and signifies the height below which the logarithmic wind profile does not hold. Stearns (1970) computed the displacement height by minimizing the sum of the squares of the errors between the wind speed observed at several heights and the wind computed from the theoretical expression for wind variation with height

In this model, Z_d is not treated as a constant, but is computed for each data set. It is regarded as a function of the stability parameter, represented by the gradient Richardson number, Ri.

$$Ri = \frac{g\,(\Delta T)\,(\Delta z)}{T_m\,(\Delta U)^2} \qquad \ldots\ldots\ldots(2.1)$$

Where $\Delta T = T_2 - T_1$; $\Delta U = U_2 - U_1$; $T_m = T_1 + 273.0$; $\Delta z = z_2 - z_1$

Unstable case : In this case the non-dimensional wind shear, as a function of Ri, is expressed as :

$$\phi_m(Ri) = (1.0 - C_1 Ri)^{-1/4} \qquad \ldots\ldots\ldots(2.2\ a)$$

Define $C_1 = (U_1 U_2)^{1/2}/\Delta U\ .\ (z_2 / z_1)$ and $\delta = C_1\ .(U_1 / U_2)$ ..... .(2.2 b)

If $\phi_m(Ri_d)$ represents the non-dimensional wind shear at the displacement height, where the Richardson number is Ri_d, then the ratio of the two wind shears is assumed to be given by the following expression :

$$\frac{\phi_m(Ri_d)}{\phi_m(Ri)} = (1.0 + \delta\,|Ri|)^{1/4} \qquad \ldots\ldots\ldots(2.3)$$

Stable case: In this case, the non-dimensional wind shear is expressed as :

$$\phi_m(Ri) = 1.0 + C_1\, Ri \qquad \text{.....(2.4 a)}$$

where C_1 is given as in Eq.(2.2 b)

The ratio of the non-dimensional wind shears is given by the following expression:

Define $\delta = (U_1/U_2)^4$ ....(2.4 b)

$$\frac{\phi_m(Ri_d)}{\phi_m(Ri)} = (1.0 + \delta\, Ri)/\phi_m(Ri) \qquad \text{.....(2.5)}$$

Having obtained the values of $\phi_m(Ri_d)$ from Eqs. (2.3) or (2.5), Ri_d can be obtained as follows

$$Ri_d = \begin{cases} (1.0 - 1.0/[\phi_m(Ri_d)]^4)/C_1 & Ri < 0.0 \\ (\phi_m(Ri_d) - 1.0)/C_1 & Ri > 0.0 \end{cases}$$

Obukhov (1971) expressed the Richardson number as:

$$Ri = z\,\frac{k\,g\,H/(\rho C_p)}{\alpha\, u_*^3}\,\{\phi_m(Ri)\}^{1/2}$$

$$\left.\frac{\partial Ri}{\partial z}\right|_{z\to 0} = -\frac{k\,g\,H/(\rho C_p)}{\alpha\, u_*^3} = \frac{Ri}{z} \qquad \text{.....(2.6)}$$

At $z \to 0$ $\phi_m(Ri) \to 1$

Close to the surface , Ri can be expressed as:

$$Ri = Ri_d + \frac{\partial Ri}{\partial z}(z_m - Z_d) \qquad \text{.....(2.7)}$$

Applying Eq.(2.6) for $z=Z_d$, the expression for the displacement height becomes:

$$\boxed{Z_d = z_m(Ri_d/Ri)} \qquad \text{.....(2.8)}$$

(b) *Monin – Obukhov stability length "L"*

This is the most important parameter of the SL and all the other turbulence parameters are functions of the non-dimensional parameter (z/L). The gradient Richardson number can be expressed as:

$$Ri = \frac{\phi_H(z/L)}{[\phi_M(z/L)]^2}\,\frac{z}{L} \qquad (2.9)$$

Unstable Case

Businger's expressions for the non-dimensional wind and temperature shears are as follows:

$$\phi_M(\xi) = (1.0 - \gamma_1 \xi)^{-1/4}; \quad \phi_H(\xi) = \gamma_4 (1.0 - \gamma_2 \xi)^{-1/2} \qquad \ldots\ldots(2.10)$$

where γ_1, γ_2 and γ_4 are the "constants" to be evaluated. Substituting Equation (2.10) in (2.9) and rearranging, the following cubic equation in "ξ"is obtained:

$$\gamma_1 \xi^3 - \xi^2 - \gamma_2 \xi C_k^2 + C_k^2 = 0 \qquad \ldots\ldots(2.11)$$

where $C_k = Ri / \gamma_4$. The above equation can be solved by Cardano's method, as shown in Appendix – 1. The final solution is given by :

$$\boxed{\xi = |Ri|(Ri/3 - 1)/(1 + Ri)} \qquad (2.12)$$

Stable Case

In the stable case the non-dimensional profile functions for momentum and heat are defined as follows:

$$\phi_M(\xi) = 1 + \gamma_3 \xi; \quad \phi_H(\xi) = \gamma_5 + \gamma_3 \xi \qquad (2.13)$$

$$\gamma_5 = \begin{cases} [(1 - \sqrt{Ri})/(1 + \sqrt{Ri})]^{1/2} & \\ [(1 - Ri)/(1 + Ri)] & \end{cases} \qquad \gamma_3 = \begin{cases} 0.25\gamma_5/Ri & 0.03 < Ri < 0.1 \quad (2.14a) \\ \gamma_5\sqrt{\gamma_5}/Ri & Ri > 0.1 \quad (2.14b) \end{cases}$$

$$\gamma_5 = [(1 - Ri)/(1 + Ri)] \qquad \gamma_3 = (\gamma_5)^4/\sqrt{Ri} \qquad Ri < 0.03 \qquad (2.14c)$$

Substituting these values of $\phi_M(\xi)$ and $\phi_H(\xi)$ in Eq.(2.9) and rearranging, we get the following quadratic equation in ξ :

$$\gamma_3(\gamma_3 Ri - 1)\xi^2 + (2\gamma_3 - \gamma_5)\xi + Ri = 0 \qquad (2.15)$$

The solution of this equation is given by :

$$\boxed{\xi = -\frac{(2\gamma_3 Ri - \gamma_5)}{2\gamma_3(\gamma_3 Ri - 1)} \pm \frac{[(2\gamma_3 Ri - \gamma_5)^2 - 4\gamma_3 Ri(\gamma_3 Ri - 1)]^{1/2}}{2\gamma_3(\gamma_3 Ri - 1)}} \qquad (2.16)$$

For the condition $0.03 < Ri \leq 0.1$, the solution becomes :

$$\boxed{\xi = \frac{\sqrt{\gamma_5}}{\gamma_3(2 + \sqrt{\gamma_5})}} \qquad (2.17)$$

(c) *Turbulent velocity and temperature scales*

The non-dimensional wind shear is given by :

$$\phi_M(\xi) = kz / u_* . (\partial u/\partial z) \qquad (2.18a)$$

Hence $$\Delta u = u_* / k \int_{\xi 0}^{\xi} \phi_M(\xi) / \xi \, d\xi \qquad (2.18b)$$

The non-dimensional temperature shear is given by:

$$\phi_H(\xi) = z / T_* . (\partial T/\partial z) \qquad (2.19a)$$

Hence $$\Delta T = T_* \int_{\xi 0}^{\xi} \phi_H(\xi) / \xi \, d\xi \qquad (2.19b)$$

Unstable Case:

Substituting the expression for $\phi_M(\xi)$, as given in Eq.(2.10), in Eq.(2.28a) and integrating with respect to ξ, we get the analytical expression for the wind at any height z, as follows:

$$u = \frac{u_*}{k}\left[\ln\left\{\frac{1-\phi_M(\xi)}{1+\phi_M(\xi)}\right\} - \ln\left\{\frac{1-\phi_M(\xi_0)}{1+\phi_M(\xi_0)}\right\} + 2\tan^{-1}\{(\phi_M(\xi))^{-1}\} - 2\tan^{-1}\{(\phi_M(\xi_0))^{-1}\}\right] \qquad (2.20)$$

From this equation, u_*, can be obtained if the wind at the lowest level of observation (2m. at Kansas) is substituted for u. Initially, the value of z_0 is unknown. Therefore, the difference in the wind speeds at the two lowest levels of observation (2m and 4m at Kansas) is considered for evaluating the value of u_*. The function $\phi_M(\xi)$ is also evaluated at these two levels. With this value of u_*, the roughness height can be computed as shown in the next section. In the same way, substituting the expression for $\phi_H(\xi)$ from Eq.(2.10), in Eq.(2.19b) and integrating with respect to ξ, we get the difference between the temperatures at a height z and at the roughness height z_{oT} for temperature, as follows:

$$\Delta T = \gamma_4 T_* \left[\ln\left\{\frac{\phi_H(\xi_0) - \gamma_4}{\phi_H(\xi_0) + \gamma_4} . \frac{\phi_H(\xi) + \gamma_4}{\phi_H(\xi) - \gamma_4}\right\}\right] \qquad (2.21)$$

In this case also, initially, the temperatures at the two lowest levels of observation are considered for evaluating T_*. With this value of T_*, the roughness height for temperature is computed, as shown in the next section.

Stable Case:

Substituting the expression for $\phi_M(\xi)$, as given in Eq.(2.13), in Eq.(2.18a) and integrating with respect to ξ, we get the analytical expression for the wind at any height z, as follows:

$$u = \frac{u_*}{k}\left[\ln\left\{\frac{\xi}{\xi_0}\right\} + \gamma_3 (\xi - \xi_0)\right] \qquad (2.22)$$

Similarly, by substituting the expression for $\phi_H(\xi)$, as given by Eq.(2.13), in Eq.(2.19b) and integrating with respect to ξ, we get the expression for the temperature difference between the height z and the roughness height for temperature z_{0T}, as follows:

$$\Delta T = T_*\left[\gamma_5 \ln\left\{\frac{\xi}{\xi_0}\right\} + \gamma_3 (\xi - \xi_0)\right] \qquad (2.23)$$

As in the unstable case, the initial values of u_* and T_*, are obtained by considering the

wind speeds and temperatures at the two lowest observing levels.

(d) *The roughness heights z_0 and z_{0T}*

The roughness heights for both, momentum and temperature, are obtained by iteration. In the case of momentum, an initial guess value for z_0 is substituted for ξ_0 in Eq.(2.20) or Eq.(2.22), depending upon stability. The new value for u_* is obtained, by considering the wind speed at the lowest height (2m.) only. If this value of u_* is greater than the initial value, then the value of z_0 is altered by a small amount and the entire process repeated, until the new value of u_* is equal to, or lesser than the initial value. At this stage, the value of z_0 gave the required roughness height. The above operation follows from the fact that, very close to the surface, the stress can be considered constant and equal to its surface value.

Next, the temperature difference, ΔT_1, between the temperatures at heights of z_0 and z_1, is computed from Eqs.(2.21) or (2.23), depending upon stability. The temperature at z_0 is obtained from the relation:

$$T(z_0) = T_1 - \Delta T_1 \qquad (2.24)$$

The roughness height for temperature is obtained from the assumed relation :

$$\ln(z_0 / z_{0T}) = 2.2 \qquad (2.25)$$

The above relation was found to be valid by several authors, e.g. Garratt and Pielke (1989).

We now attempt to find a factor, η, which when multiplied by ΔT_1, gives the difference between the true surface temperature, i.e. the temperature at $z = z_{0T}$ and temperature at $z = z_1$. An initial guess for η is made and the corresponding temperature difference ΔT, is inserted in Eq.(2.21) or Eq.(2.23), to obtain the value of T_*. If this value is less than the initial value of T_*, then η is altered and the process repeated, until the value of T_* is greater than, or equal to, its initial value. The surface temperature is computed as follows:

$$T_S = T_1 - \Delta T_1 \qquad (2.26)$$

(e) *Surface Heat Flux*

The surface heat flux, H, is obtained from the following expression:

$$H = -\rho c_p k u_* T_* \qquad (2.27)$$

in units of Wm^{-2}. The observed 15-min. averaged values of heat fluxes were obtained from the covariances [w'u'], which were measured by fast-response sensors mounted at 5.66m., 11.31m., and 22.63m. The heat flux at a height of 5.66m. was converted to units of Wm^{-2} for comparison with the computed values.

(f) *Depth of the surface boundary layer and coefficient of eddy viscosity K_M*

The stress at a particular height z is given by the following relation:

$$\tau = \rho K_M (\partial u/\partial z) \qquad (2.28)$$

Expressing $(\partial u/\partial z)$ in terms of the function $\phi_M(\xi)$, from Eq.(2.18a), we get :

$$\tau/\tau_0 = K_N \phi_M(\xi) / \xi \qquad (2.29)$$

where $\tau_0 = \rho u_*^2$ and $K_N = K_M/(k u_* L)$

The SL is defined as the layer close to the surface where the stresses are almost constant with height. If we define the top of the SL as the height where $\tau/\tau_0 = \delta$, δ being a fraction close to one, then it is possible to solve Eq.(2.39) and obtain the depth of the SL, provided the value of K_N is known. Zilitinkevich and Laykhtman (1965), have

expressed K_N for unstable stratification as follows:

$$K_N = 1 - y^4 \qquad (2.30)$$

where y is a non-negative variable related to ξ as follows:

$$\xi = 2/y - 2y^3/3 - 4/3 \qquad (2.31)$$

Starting with a guess value for y in Eq.(2.31), we solve Eq.(2.30) by the Newton-Raphson method until the appropriate value of ξ is obtained, from which the depth of the SL is computed. The depth of the SL can also be computed from the empirical relation :

$$h_1 = -(\gamma_1 L/\gamma_2)(1 - Ri) \qquad (2.32)$$

In stable stratification, certain empirical relationships are assumed between ξ and ϕ_M at the top of the SL, for two categories of turbulence. The turbulence characteristic is defined in terms of the Ri-number. The two categories of turbulence are defined as follows:

$$0.04 < Ri < 0.19 \quad \xi = 1/[\phi_M(\xi)]^2 \qquad (2.33a)$$

$$Ri < 0.04 \quad \xi = 1/\gamma_3 \qquad (2.33b)$$

Eq.(2.33a) can be expanded to : $\gamma_3^2 \xi^3 + 2\gamma_3 \xi^2 + \xi - 1 = 0$. This cubic is solved to give the value of ξ at the top of the SL, from which the depth of the SL can be evaluated.. The empirical expression for obtaining the depth of the SL is given by:

$$h_1 = L(1 - Ri)/\gamma_3 \qquad 0.04 < Ri < 0.19 \qquad (2.34a)$$

$$h_1 = L(1 - Ri)/\gamma_3/\gamma_5 \qquad Ri < 0.04 \qquad (2.34b)$$

Figure (5a) shows the variation of the ratio (h/h_1) with Ri-number. This ratio is close to unity, except for values of Ri-number close to zero..
Figure (5b) shows the variation of h with Ri-number and reveals a gradual increase in the depth of the SL with the approach towards neutral stratification. The depths in unstable stratification are much larger than in stable stratification.

The coefficient of eddy viscosity within the SL can also be obtained. In unstable stratification, Eqs.(2.30) and (2.31) give the value of K_N at different values of z ,from which the coefficient K_M can be obtained. Figure (6a) gives the variation of K_M with height, for three different values of the Ri-number. It is seen that for stronger instability, characterized by higher values of the stability length L and Ri-number, the slope of the curve is lesser, indicating lower magnitudes of the eddy viscosity at a particular height. In stable stratification, the value of K_M at any height z, is obtained from the equation: .
$K_M = k u_* z / \phi_M(\xi)$

The correctness of the computed values of K_M was checked with the observed values of [u'w'] at a height of 5.66m. The value of K_M was converted to the stress form, using Eq.(2.39), as follows:

$$[u'w']_{com} = K_M u_* \phi_M(\xi)/(kz) \qquad (2.36)$$

where z = 5.66 and ξ is calculated for the same height Figure (6b) shows the variation of the ratio of the computed stress to the observed stress, with ξ, all the parameters being calculated for z = 5.66m. It may be seen that the mean value of the ratio is 0.876, which is close to unity, suggesting that the computed values of τ/ρ are very nearly equal to the observed values at z = 5.66m.

3. Discussion

(a) *Displacement Height* : The validity of the assumed expressions represented by Eqs.(2.3) and (2.5), is tested by considering the layers between the following heights: (1)

2m to 4m (2) 4m to 8m. The Richardson numbers and also the constants C_1 and δ are computed for the two layers. The original versions of the expressions represented by Eqs(2.3) and (2.5), which were used in this test, are as follows:

$$\frac{\phi_m(Ri_1)}{\phi_m(Ri_2)} = (1+\delta\,|Ri_1|)^{1/4} * (1 + Ri_1) \qquad \text{(Unstable)} \ldots. \quad (3.1)$$

$$\frac{\phi_m(Ri_1)}{\phi_m(Ri_2)} = (\phi_m(Ri_1) + \delta\, Ri)/\, \phi_m(Ri_2) \qquad \text{(Stable)} \ldots\ldots. \quad (3.2)$$

Here, Ri_1 and Ri_2 are the Ri-numbers in the lower and upper layer, respectively. At the level of the Z_d the function $\phi_m(Ri)$ can be taken as unity, which is the value used in Eqs.(2.3) and (2.5) and the same is the case for the factor $(1 + Ri_1)$.

Figure 1, shows a plot between the ratio of the *left hand side* to the *right hand side* of equations (3.1) and (3.2), and the Ri-number. It may be seen the ratio is very nearlyly equ to unity for all values of Ri-number, thus confirming the validity of Eqs. (3.1) d and (3. and hence, equations (2.3) and (2.5), respectively.

Figure 2 shows the variation of Z_d with Ri. In unstable stratification (-ve values of Ri) the displacement height increases with an increase in Ri. An increase in Ri dicatesi i the tendency towards a less unstable stratification and thus, a decrease in the intensity of turbulence and an increase in the turbulent velocity and length scales. In n stab stratification, there is little variation of the displacement height with Ri.

(b) *Profile function "constants" and turbulent Prandtl number*: Figure(4a) shows the variation of the factor "f" and the "constant" γ_4(GM4), with Ri . It is seen that γ_4 increases with increasing Ri, whereas, "f" decreases with increasing Ri. At Ri = -0.223, $f = \gamma_4$, suggesting that this value gives the critical Ri- number, which demarcates the logarithmic regime from the diabatic regime in the SL.. Thus, in the range $-0.223 < Ri < 0$, the value of " f " can be directly obtained from the relation $\{|Ri|^{1/4}\}/ f = 1$, and the values of the "constants" $\gamma_1, \gamma_2, \gamma_4$, can be obtained from Eq.(2.19). The value of α can also be directly obtained. Figure (4b) shows a plot between the variable "constants", γ_1 and γ_2 as a function of Ri-number. It shows increasing values with increasing Ri-numbers.

We now define a new parameter as: $\alpha_1 = \gamma_1 /(\gamma_2\, \gamma_4)$ and another parameter as : $C = \{|Ri|^{1/4}\}/ f$. Figure (8a) gives a plot of the parameter C and the product $\alpha_1 * C * TPr$, against the Richardson number. It may be seen that at the value Ri = -0.223, both C and the product parameter have the same value of unity, suggesting that at this value of Ri the parameter α_1 can be expressed as the inverse of TPr. It is known that α is equal to the inverse of the TPr in a logarithmic boundary layer and therefor, $\alpha_1 = \alpha$ at this value of Ri-number, which also marks the beginning of the logarithmic boundary layer regime. For higher values of Ri (lower magnitudes of Ri), the two curves almost coincide with each other, indicating the validity of the equality $\alpha_1 = \alpha = 1/TPr$. For lower values of Ri (higher magnitudes of Ri), in Figure (8a), the parameter C decreases, whereas the product parameter remains almost constant at a value very close to unity, suggesting that in this region of stability, C gives the deviation from the logarithmic condition

Figure (8b) gives the variation of TPr and the product $(\alpha_1 * TPr)$, with Ri- number. If

we neglect the energy diffusion term in the turbulent kinetic energy equation, it can be shown that the criterion for the existence of non-damping turbulence is given by: $Ri < TPr$. It may be seen from the figure that this criterion is satisfied for $|Ri| < 0.4$. Thus, beyond this value of Ri, the turbulent kinetic energy gets damped. The turbulent Prandtl number characterizes the convective motion in the turbulent convective layer in a fluid and it gives the relative magnitudes of momentum and heat diffusivity. The figure shows that TPr varies almost linearly with Ri-number, increasing towards lower magnitudes of Ri. The eddy sizes are inversely proportional to the dominant wave numbers of convection and mechanical turbulence and mechanical eddies are known to have smaller wavelengths (larger wave numbers) than eddies produced by heating. Heat is transported more efficiently by the larger eddies.

(c) *Comparison of the solution, ξ, with the iterative method :* The solution , ξ, is also computed iteratively, using Businger's profile functions and constants, which had the following constant values, viz.: $\gamma_1 = 16$, $\gamma_2 = 9$, $\gamma_3 = 4.7$, $\gamma_4 = 0.74$. The roughness heights for momentum and temperature, were kept constant as $z_0 = 2.4$ cms. Figure (7a) shows the variation of the ratio of the solution obtained by this method(SL), to that obtained by the iterative method(SL1), with Ri-number,for unstable stratification. It is seen that the ratio increases towards higher values of Ri-number. Figure (7b) shows the variation of the ratio of α(ALP) , obtained by this method, to that obtained by the iterative method(ALP1), with Ri-number. This ratio also increases towards higher values of Ri-number. In the case of stable stratification
the variation of the solution ratios are not smooth as in the previous case, but show discontinuities at the boundaries where the stability regimes changes by definition. For values $Ri > 0.2$, the iterative solution does not converge and measurements in the atmosphere made by several authors, indicate that turbulence is not found above a value of $Ri = 0.2$.

(d) *Comparison of the friction velocity , surface heat flux and Monin-Obukhov Stability length with observed values :* The parameters u_*, H and L were computed and compared with the observed values. The 15-minute averaged covariances [u'w'] and [θ'w'] from the fast response sonic anemometer at a height of 5.66m., were used for computing the observed values of u_*, H and L. These parameters were also computed by the Direct solution method and Businger's profile functions, using his constants. The fractional percentage departure of the computed values from the observed values were computed as follows :$\text{Error(ust)}=\{u_* - (u_*)_{obs}\}/(u_*)_{obs} \cdot 100$ $\text{Error(ol)}=\{L-(L)_{obs}\}/(L)_{obs} \cdot 100$, $\text{Error(hf)}=\{H-(H)_{obs}\}/(H)_{obs} \cdot 100$. Figures (9a,b,c) give a plot of these percentage departures as a function of the Ri-number, for the direct solution method. It may be seen that the percentage departures are distributed about the zero value, with a slight weight towards negative departures in the case of friction velocity and heat flux, indicating that the computed values are underestimated in comparison with the observed values in more cases. This may be due to the fact that the covariances are more pronounced at a height of 5.66m. than at the height of 2m. or 4m. and, therefore, the fluxes computed from these covariances tend to give higher values than those computed by the direct solution method. Similar fractional percentage departures were also computed by using Businger's iterative solution method and the logarithm of the ratio of the departures by the direct method, to this method, were computed. Figures (9d,e,f) give a plot of this ratio, as a function of Ri-number. Negative values of the ratio indicate that the percentage departures by the iterative method is larger than those obtained by the direct method. Both the methods appear comparable in regard to the percentage departures from observed values.

(e) *Comparison of wind and temperature profiles constructed from computed surface parameters* : The values of L, u_* and T_*, computed by this method and by the iterative method using Businger's constants, were used to construct the vertical profiles of wind and temperature. The computed values at each standard height, were compared with the observed values at that height and the "difference" computed. The difference is expressed as a percentage of the observed values. The mean wind and temperature differences were computed for each level of observation and for each method of computation. Method A is the direct solution method, method B is Businger's iterative method with variable values of the surface roughness parameters for wind and temperature, respectively, while method C is also Businger's iterative method , but with fixed values of the surface roughness parameters. In method C, the roughness parameter for wind and temperature are given the same value. The percentage differences for wind are expressed by ERRU(A), ERRU(B), ERRU(C), for each of the aforesaid methods A,B,C respectively, whereas the temperatures differences are expressed by TERR(A), TERR(B), TERR(C). Figure (10a) gives the mean percentage wind differences for each level of observation and for each method, along with the associated standard deviations. The computed values are for unstable stratification and for those data samples for which the level of observation is within the surface layer, i.e. the ratio SLH/Z > 1, where SLH indicates the height of the surface boundary layer and Z is the height of the observation level. The observation levels are at heights of 2m, 4m, 8m, 16m, 22.63m and 32m. respectively. It is seen that the relative percentage differences and the respective standard deviations are slightly larger in method C, as compared with the other methods.

Figure (10b) shows the same parameters for the percentage temperature differences. The mean differences and the respective standard deviations appear to be almost the same for all the three methods, suggesting the insensitivity of the variable profile "constants" and the roughness parameters to change the temperature profiles, in the statistical sense. The computed surface temperatures probably adjusts to the variable profile constants and roughness parameters, to yield almost the same vertical profile.

Figure (11a,b) show the same parameters for unstable stratification, but in the case, where the height of the observation level is greater than the height of the surface layer, i.e SLH/Z < 1. It is seen that the mean percentage differences at each level of observation, for both wind and temperature, are much higher compared with the values in Figure (10a,b), except for method C, where no significant change is noticed. The standard deviations are also much higher in methods A and B, respectively. It is known that the similarity hypothesis is strictly valid in the surface boundary layer only and the larger percentage differences between the observed and the computed parameters in the range beyond the height of the surface boundary layer, is a reflection of this fact. It is probable that the height of the SL, as computed in methods A and B, may not be valid for method C and so the parameters computed by the application of the similarity theory, do not show any significant change beyond the computed value of the SL height.

Figure (12a,b) show the same parameters for stable stratification and for the condition SLH/Z > 1. In this case, the mean percentage differences for wind and temperature, are nearly the same for methods A and B, but show much higher values for method C. The standard deviation also follow the same pattern. Figure (13a,b) show the same parameters for stable stratification., but for the condition SLH/Z < 1. It is seen that the mean percentage differences are much higher for all the methods, as compared with Figure (12,a,b). The standard deviations are also very large. The stable SL appears to be very sensitive to the SL height, which is not continuous, as in unstable stratification, but has discontinuities at the boundaries of each stability range.

4. Conclusion

The present model gives a very simple and accurate method of computing the M-O stability length, using data at two levels only. Since all the other parameters in the SL are some functions of the non-dimensional parameter (z/L), they too can be computed easily and accurately. The importance of computing the roughness heights for momentum and temperature for each data set, is highlighted in this model, when it was shown that the percentage differences from observed values came down appreciably, while using Businger's method, after the roughness heights were made variable, in method B, for the computation of wind profile. The model brings out an objective method for computing the displacement and the roughness heights from observed data. The criterion for evaluating the depth of the SL has also been developed, which will help in deciding the boundary beyond which the M-O similarity hypothesis is not applicable. As this model gives the solution directly, the problem of convergence does not arise and considerable time is saved compared with the method of iterations. This model can also compute the vertical profile of wind and temperature accurately, using only the data obtained at the two lowest levels.

References

Beljaars, A.C.M., and A.A.M.Holstag (1991) : Flux parameterization over land surfaces for atmospheric models. *J. Of App. Meteor.*, **30**, 327-341

Berkowicz, R. and L.P.Prahn (1982) : Evaluation of the profile method for estimation of surface fluxes of momentum and heat. *Atmos. Environ,*. **16**,.2809-2819

Businger, J.A., J.C.Wyngaard, Y.Izumi and E.C.Bradley (1971) : Flux profile relationships in the atmospheric surface layer. *J. Atmos. Sci.*, **28**, 181-189.

Businger, J.A. (1961) : On the relation between spectra of turbulence and the diabatic wind profile. *J. Geophy. Res.*, **66**, 2405

Byun,D.W. (1990) : On the analytical solutions of the flux-profile relationships for the atmospheric surface layer. *J. Of App. Meteor.* **29**, 652-657

Garratt, J.R. and R.A.Pielke (1989) : On the sensitivity of mesoscale models to surface-layer parameterization constants. *Bound. Layer. Meteor.*, **48**, 377-387

Izumi, Y. (1971) : Kansas 1968 Field Program data report. *Air Force Cambridge Res. Lab., Bedford, Mass., Report No. AFCRL –72 – 0041,* 79 pp.

Lo, Aloysius. K (1977) : An analytical-empirical method for determining the roughness length and zero-plane displacement. *Bound. Layer. Meteor.*, **12**, 141-151

Obukhov, A.M. (1971) : Turbulence in an atmosphere with a non-uniform temperature. *Bound. Layer. Meteor.*, **2**, 7-29

Pasquill, F. (1972) : Some aspects of boundary layer description. *Quar. Jour.Roy.Met.Soc.*, **98**, 469-494

Stearns, C. (1970) : Determining surface roughness and displacement height. *Bound. Layer. Meteor.*, **1**, 102-111

Tennekes, H. and J.L.Lumley (1972) : A first course in turbulence. MIT Press, Cambridge, MA, 300pp.

Zilitinkevich, S.S. and D.L.Laykhtman (1965) : Turbulent conditions in the near-surface layer of the atmosphere. *Atmos. and Oceanic Phy.,(Izv),* **1**, 90-93

APPENDIX - 1

Equation (2.11) is of the form : $a x^3 + b x^2 + c x + d = 0$,
Where $x = \xi$; $a = \gamma_1$; $b = -1$; $c = -\gamma_2 C_k^2$; $d = C_k^2$
Applying the substitution , $ax = y - b/3$, the above equation can be reduced to the form:

$$y^3 + p y + q = 0 \qquad \ldots(A1)$$

where $p = -\gamma_1 \gamma_2 C_k^2 - 1/3$; $q = (p + 1/3)(1/3 - \gamma_1/\gamma_2) - 2/27$ ..... (A2)
Eq.(A1) can be solved analytically by Cardano's method. Let $\nabla = (q/2)^2 + (p/3)^3$, where "q" is positive and "p" is negative. A real solution of Eq.(A1) exists only if $\nabla > 0$. The appropriate values of "p" and "q" have to be sought, which will satisfy this condition. A factor "f" is defined as:
$f = f_0/(1.0 + Ri)$, where "f_0" is a constant representing the value of "f" when $Ri = 0$, i.e. neutral stability. It also represents the minimum value of "f". Let $s = 1/3 - (\gamma_1/\gamma_2)$ and " q " be represented by: $q = -f p$, then from Eq.(A1) we get:
$s = (-f p + 2/27)/(p + 1/3)$

Hence, $\gamma_1/\gamma_2 = 1/3 - s$ ..(A3)
And $\gamma_1 . \gamma_2 = -(p + 1/3)/ C_k^2$ .....(A4)

It is evident that for a given value of "p", "f_0" gives the minimum value for "s" and therefore, the minimum value for the ratio (γ_1 / γ_2), because "s" is negative. Hence, in order to evaluate "f_0", the condition for this ratio to be minimum has to be derived. The optimum value of "p" has also to be chosen, which satisfies the condition, $\nabla > 0$.
If $a1 = Ri/\xi$ and $a2 = \phi_H(\xi)/[\phi_M(\xi)]^2$, then Eq.(2.9) is satisfied if $a2/a1 = 1$. Figures (3a) shows the values of ∇, for various values of "p", for two values of Ri-numbers, viz., Ri=-0.05 and Ri=-0.2, respectively. It may be seen that ∇ is maximum for a particular value of "p", for each value of the Ri-number. We now define a factor "X", which is multiplied to f^2, to give the magnitude of "p". Figure (3b) gives a plot between "X" and ∇, which is computed from the relation $p = -X.f^2$
It is seen that ∇ (DEL) is maximum for X=4.5, for each value of Ri-number. This condition can also be obtained mathematically, as shown below.

Now, $\nabla = f^2 p^2 / 4 + p^3 / 27$; $\partial\nabla/\partial p = f^2 p / 2 + p^2 / 9$
The condition for maximum/minimum value of ∇ is given by: $\partial\nabla/\partial p = 0$, which gives the value of "p" as: $p = -4.5 f^2$ (A5)
$\partial^2\nabla/\partial p^2 = f^2 / 2 + 2 p / 9$. Substituting the value of "p" given above in this equation, we get the R.H.S. as: $-f^2/2$, which shows that this value of "p" gives a maxima for the value of ∇, given by:

$$\nabla = 27 f^6/16 \qquad (A6)$$

Substituting this value of "p" in Eq.(A3) and differentiating with respect to "f", we obtain the condition for the minimum value of the ratio (γ_1 / γ_2) as:

$$243 f^3 - 54 f - 8 = 0 \qquad (A7)$$

Solving this equation by Newton-Raphson method, we get the minimum value of "f" as: $f_0 = 0.5329$. From Eqs.(A3) and (A4) we get :

$$\gamma_1 = \gamma_4 (4.5 f^3 + 1.5 f^2 - 1/27)^{1/2} / |Ri| \qquad (A8)$$

If we choose the value of γ_4 such that:

$$[\gamma_4]^{-1} = [4.5\, f^3 + 1.5\, f^2 - 1/27]^{1/2} \qquad (A9)$$

Then $\gamma_1 = 1/|Ri|$ (A10)

And $\gamma_2 = [4.5\, f^2 - 1/3]\gamma_4^2 / |Ri|$ (A11)

The "constants" in Businger's profile functions are now expressed as functions of the Richardson's number. Figure (4a) shows the variation of γ_4 and the factor "f", with Richardson's number. It may be seen that while the value of γ_4 increases with increasing values of Ri, the value of "f" decreases. γ_4 is proportional to the turbulent Prandtl number (TPr), which is known to increase with decreasing turbulence and approaches unity as the stability tends towards the neutral state. The factor "f" decreases from a value close to unity, for very low values of Ri - number, to the value f_0 as the neutral state is approached. The two curves intersect at $Ri \sim -0.223$. Figure (4b) shows a plot between the variables γ_1 and γ_2 and the Ri – number. The plot shows increasing values of γ_1 and γ_2 with increasing of Ri – number. The solution of Eq.(A1) is given as follows:

$$y = u - p/3u \qquad (A12)$$

where $u = [-q/2 + \nabla^{1/2}]^{1/3}$

Substituting the appropriate values of "q", "p" and ∇, in terms of the factor "f", we get:

$$u = f\,\frac{[3\sqrt{3} - 9]^{1/3}}{4^{1/3}} = -0.9834\, f$$

$$y = -2.5087\, f$$

$$\xi = (y + 1/3)/\gamma_1$$

Substituting the values of all the parameters in the R.H.S. we get the final solution as:

$\xi = |Ri|(Ri/3 - 1)/(1 + Ri)$ (A13)

Legends of the Figures

Figure (1) : Ratio of the L.H.S. to the R.H.S. of the Eqs.(3.1) and (3.2), respectively, against Ri-number

Figure (2) : Variation of the displacement height, Z_d, with Ri-number

Figure (3a) : Variation of "∇" (DEL), with "p", for Ri = -0.2 and Ri = -0.05

Figure (3b) : Variation of "∇" (DEL), with the factor "X", in $p=-Xf^2$, for Ri=-0.05 and Ri=-0.2

Figure (4a) : Variation of the "constant" γ_4 (GM4) and the factor "f " ,with Ri-number

Figure (4b) : Variations of the "constants" γ_1 (GM1) and γ_2 (GM2) with Ri-number

Figure (5a) : Variation of the ratio of the depth of the SL (h), obtained from the solution of the relevant equation, to the depth obtained from the empirical equation, (h1), with Ri-number

Figure (5b) : Variation of the scaled depth of the SL, obtained by the solution of the relevant equation, with Ri-number

Figure (6a) : Variation of the coefficient of eddy viscosity, K_m, with height in unstable stratification, for three values of Ri-number

Figure (6b) : Variation of the ratio of the computed surface stress to the observed stress measured at 5.66 m., with ξ

Figure (7a) : Variation of the ratio of the solution ξ obtained by this method to the solution obtained by the iterative method using Businger's constants

Figure (7b) : Variation of the ratio of "α" (ALP) obtained by this method to that (ALP1) obtained by the iterative method using Businger's constants.

Figure (8a) : Variation of the parameters C, the product $C*\alpha_1*$ TPr, and TPr, with Ri-number in unstable stratification

Figure (8b) : Variation the turbulent Prandtl number and the product α_1* TPr , with Ri-number in unstable stratification

Figure (9a) : Variation of the percentage difference of "u_*" ,with Ri-number

Figure (9b) : Variation of the percentage difference of "L", with Ri-number

Figure (9c) : Variation of the percentage difference of "H", with Ri-number

Figure (9d) : Variation of the logarithm of the ratio of the percentage difference of "u_*" , computed by the direct method to that computed by the Businger's iterative method, with Ri-number

Figure (9e) : Same as in Figure (9d), but in respect of the stability length "L"

Figure (9f) : Same as in Figure (9d), but in respect of the heat flux "H".

Figure (10a) : Variation of the mean percentage difference of the wind computation at each data level, from the observed values at that level, for each method of computation, for unstable stratification. A – direct solution method. B - Businger's iterative solution with variable roughness heights for momentum and temperature. C – Businger's iterative solution with fixed roughness parameters. The vertieal lines indicate the standard deviations. The condition $h/z > 1$ holds.

Figure (10b) : Same as in Figure (10a) , but for temperature

Figure (11a,b) : Same as in Figure (10a,b), except for the condition $h/z < 1$

Figure (12a,b) : Same as in Figure (10a,b) , for stable stratification.

Figure (13a,b) : Same as in Figure (11a,b) , for stable stratification

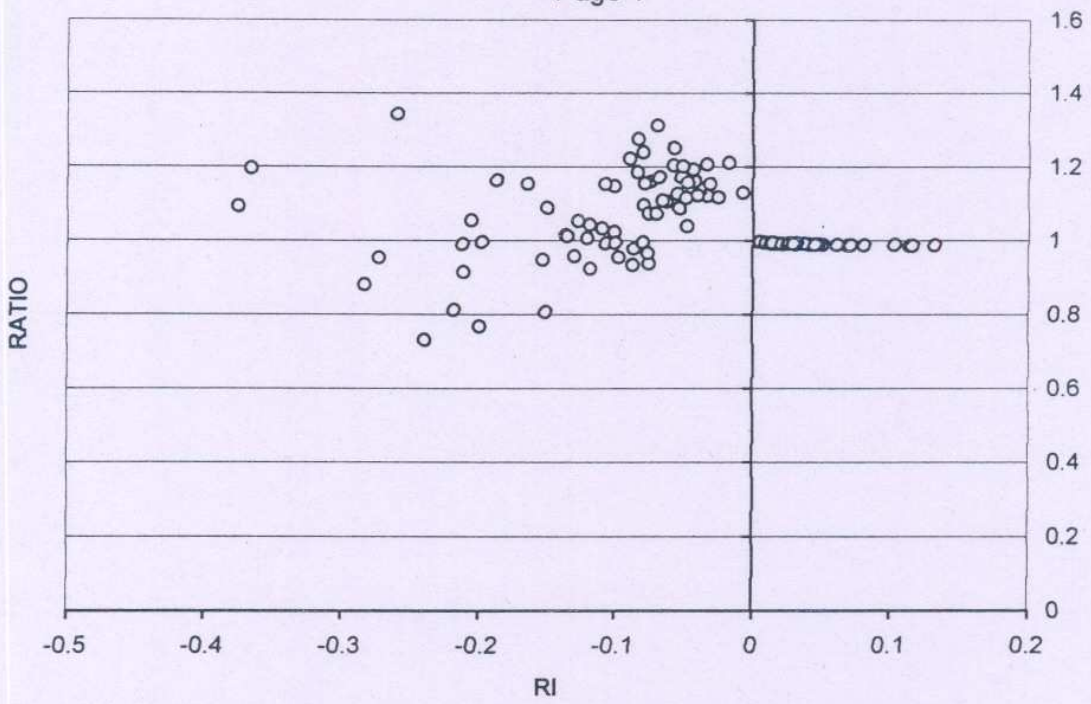

Figure 1

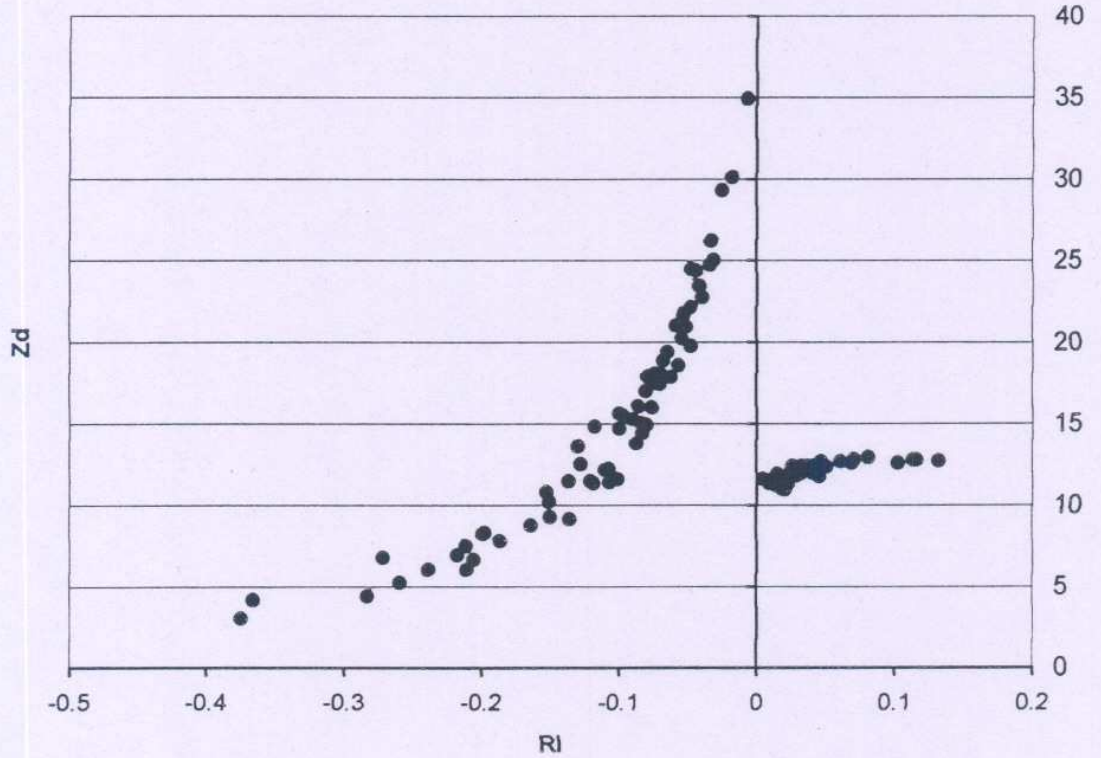

Figure 2

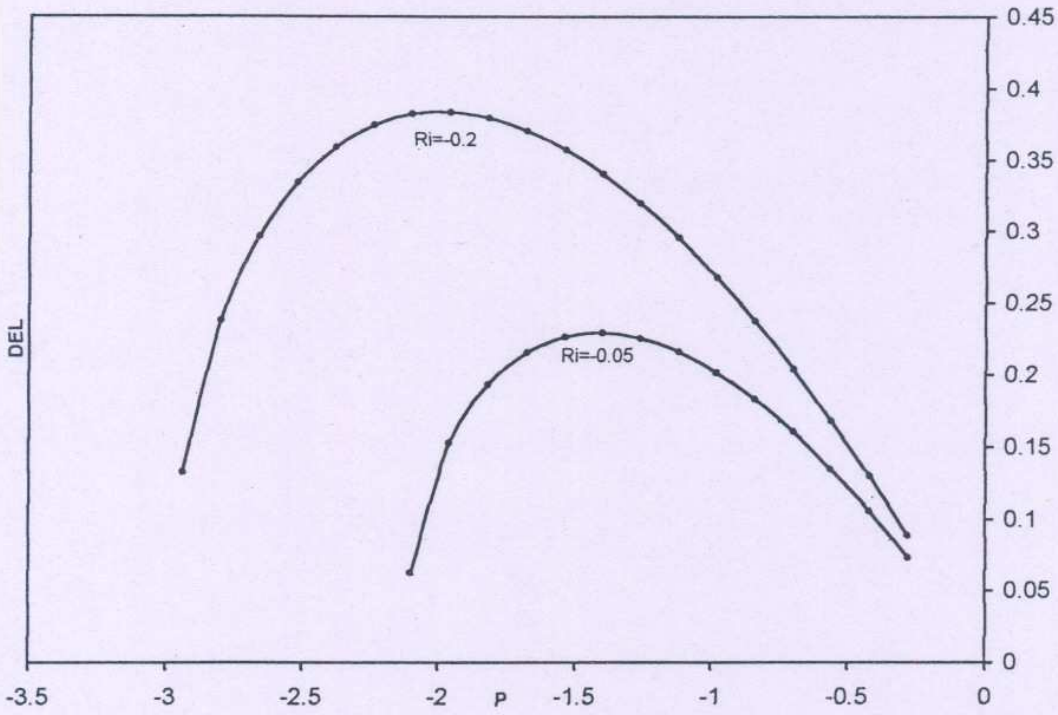

Figure 3(a)

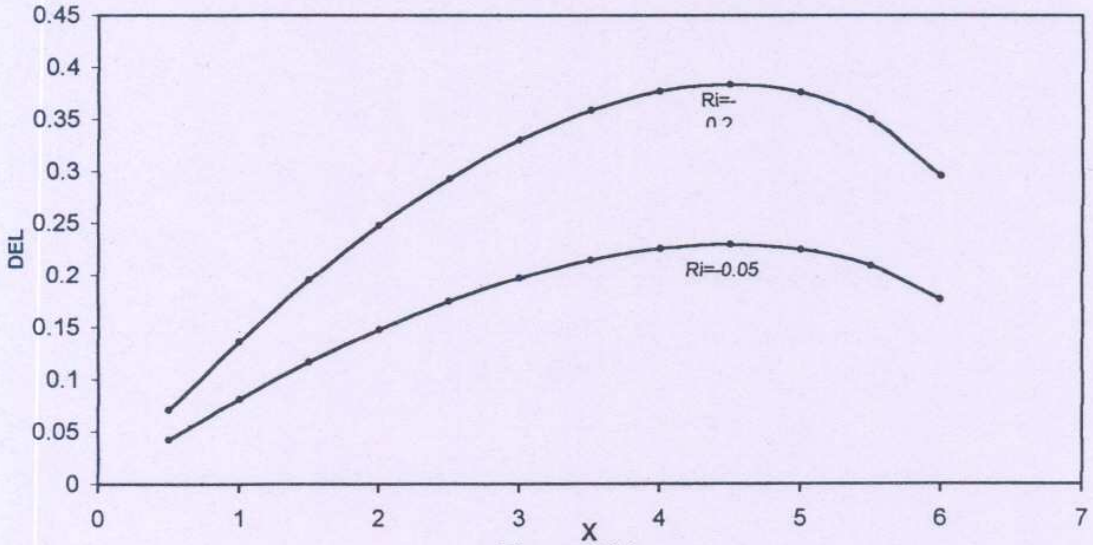

Figure 3(b)

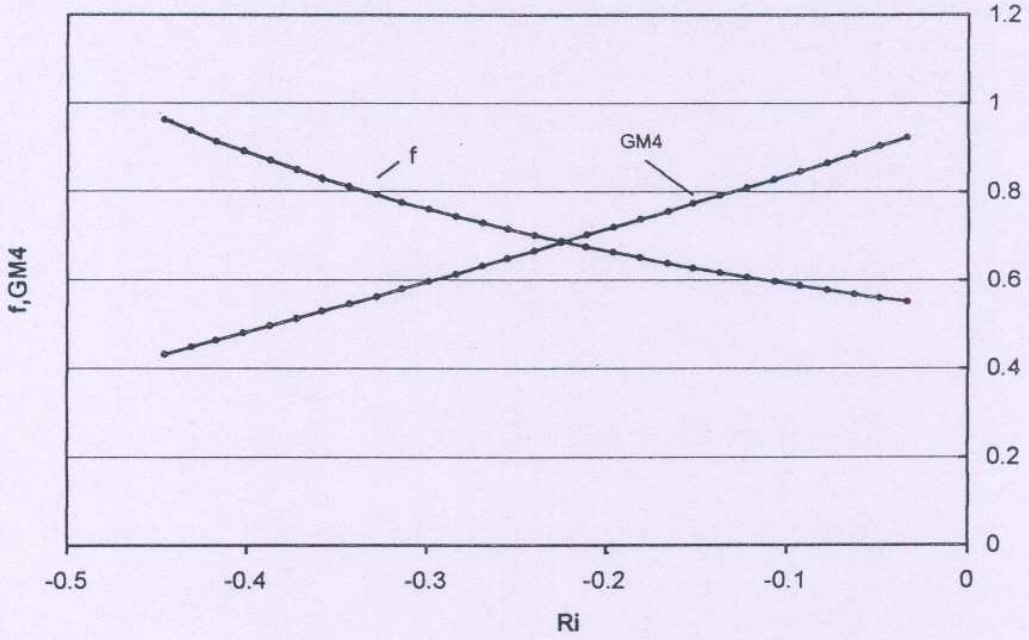

Figure 4(a)

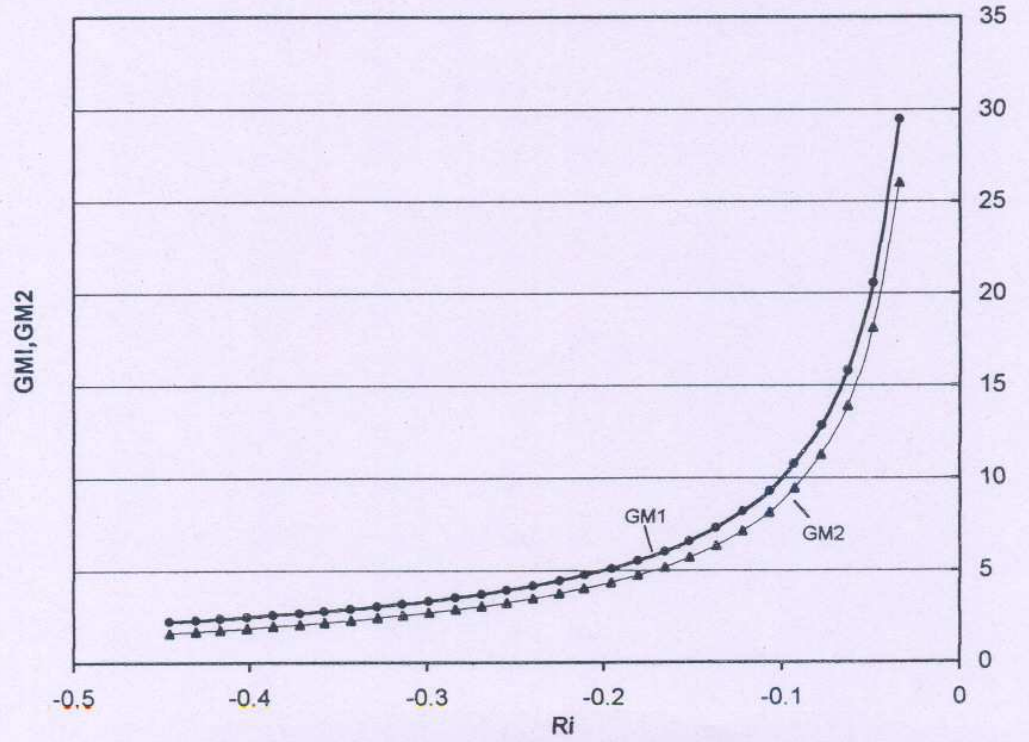

Figure 4(b)

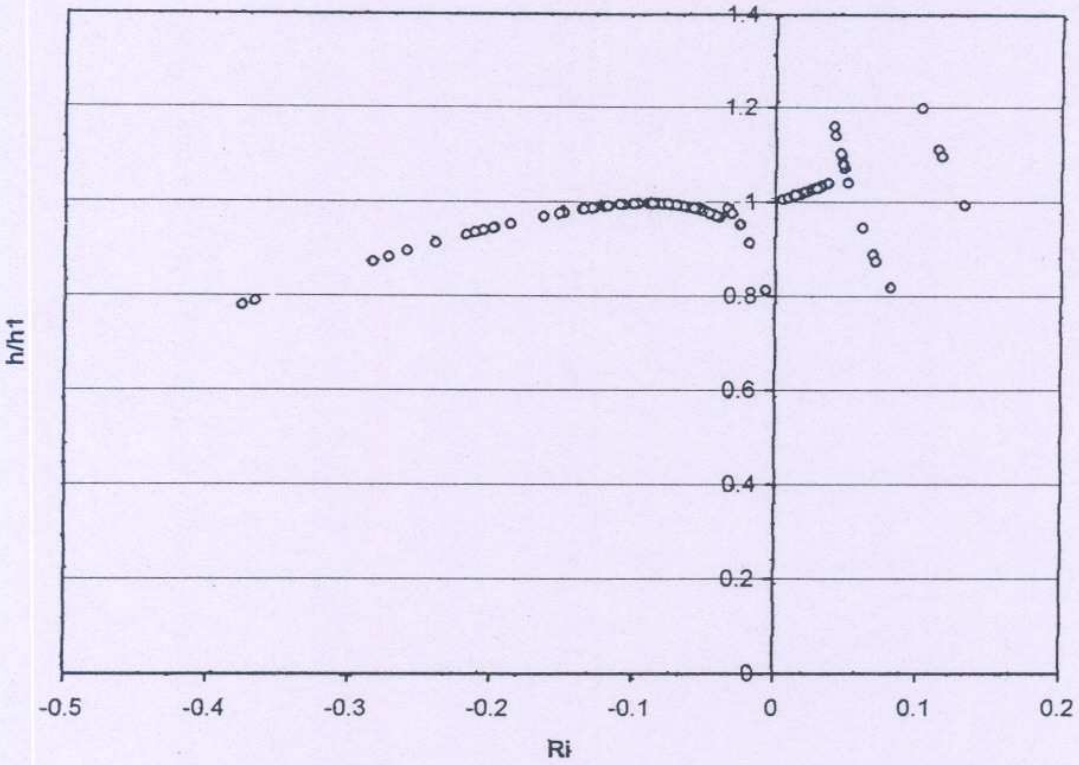

Figure 5(a)

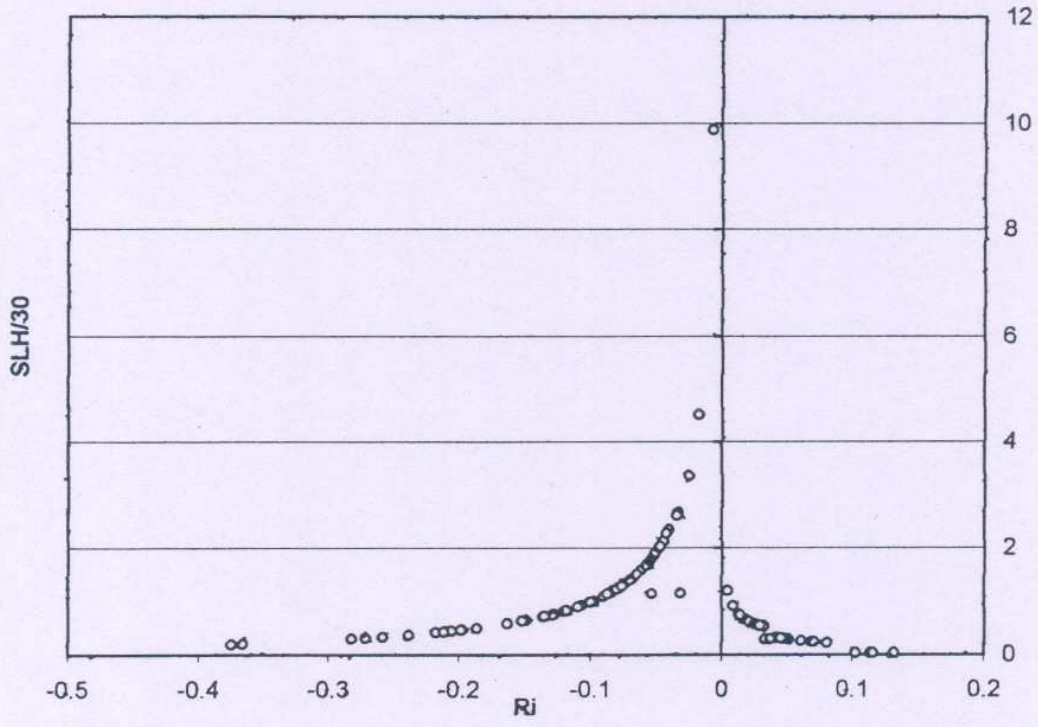

Figure 5(b)

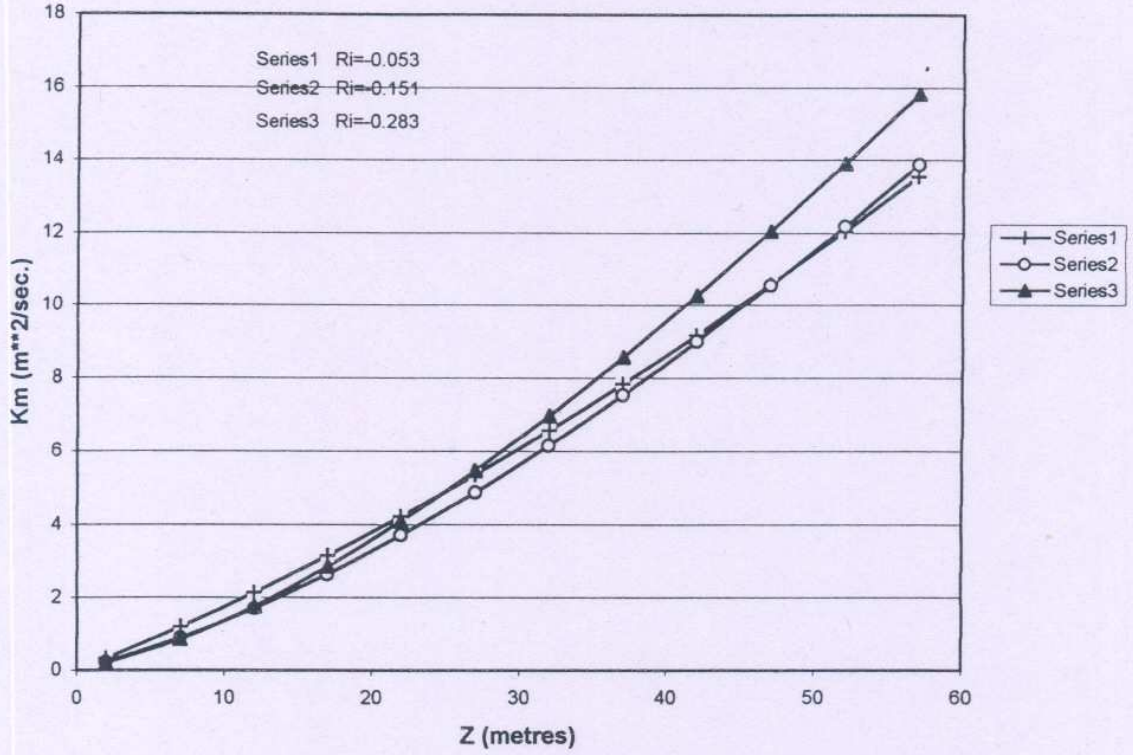

Figure 6(a)

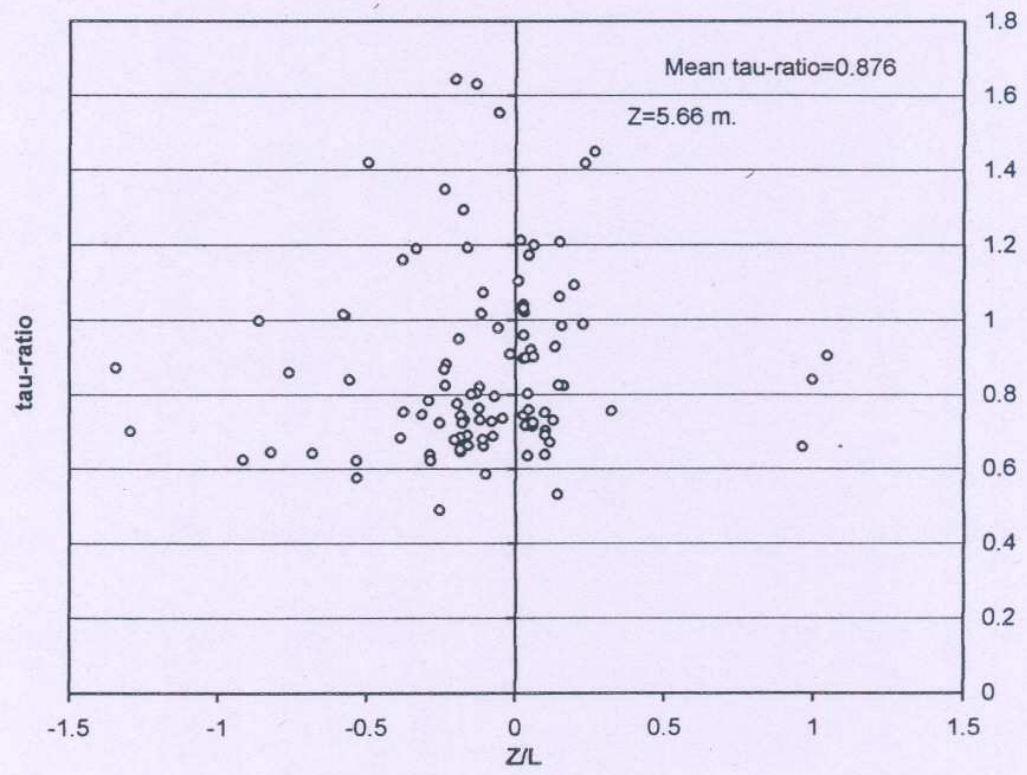

Figure 6(b)

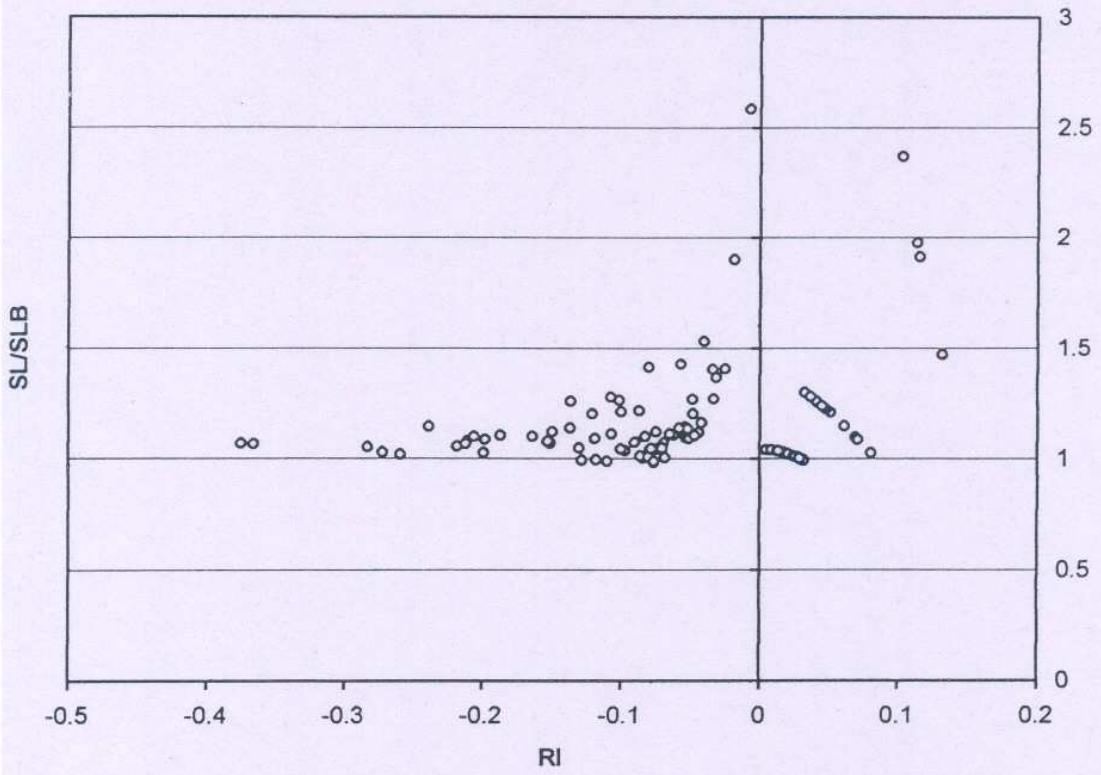

Figure 7(a)

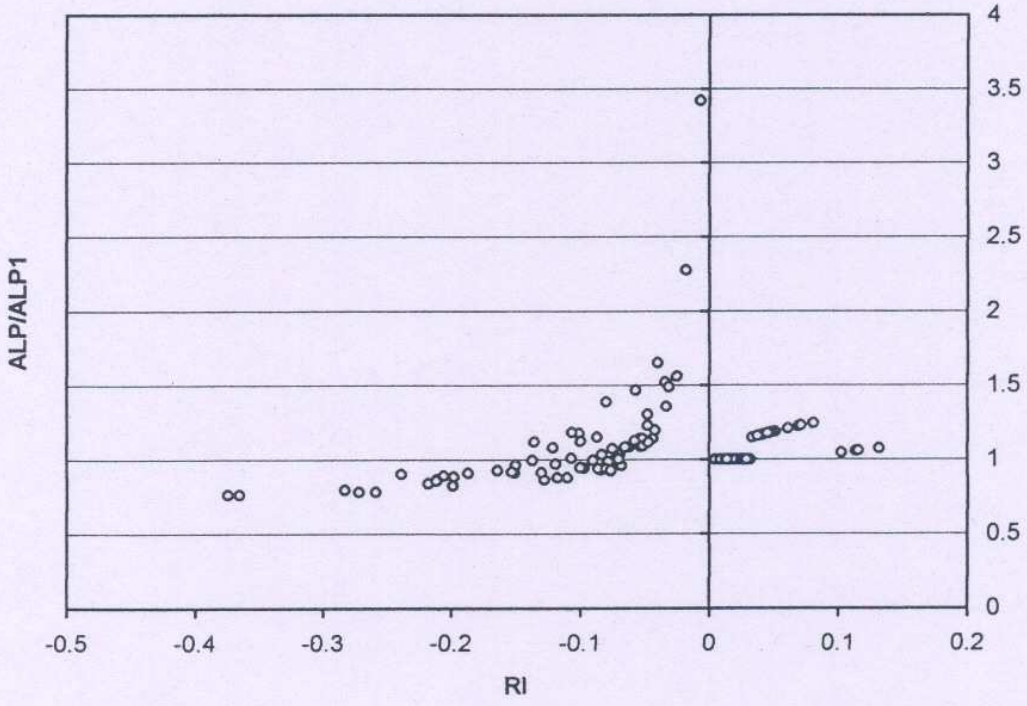

Figure 7(b)

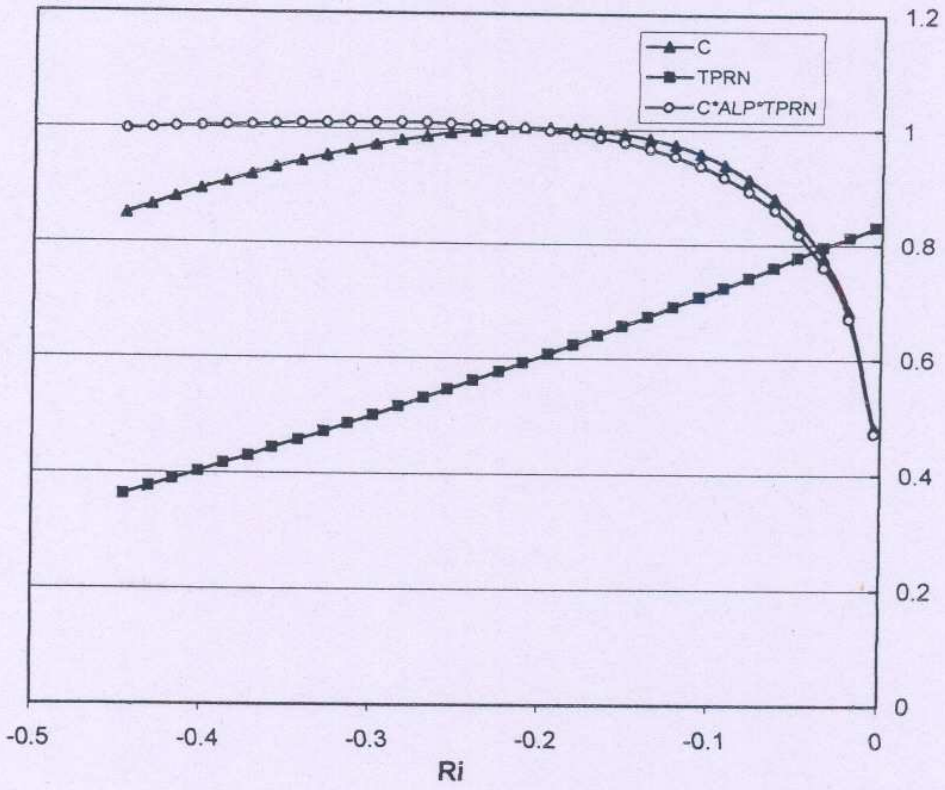

Figure 8(a)

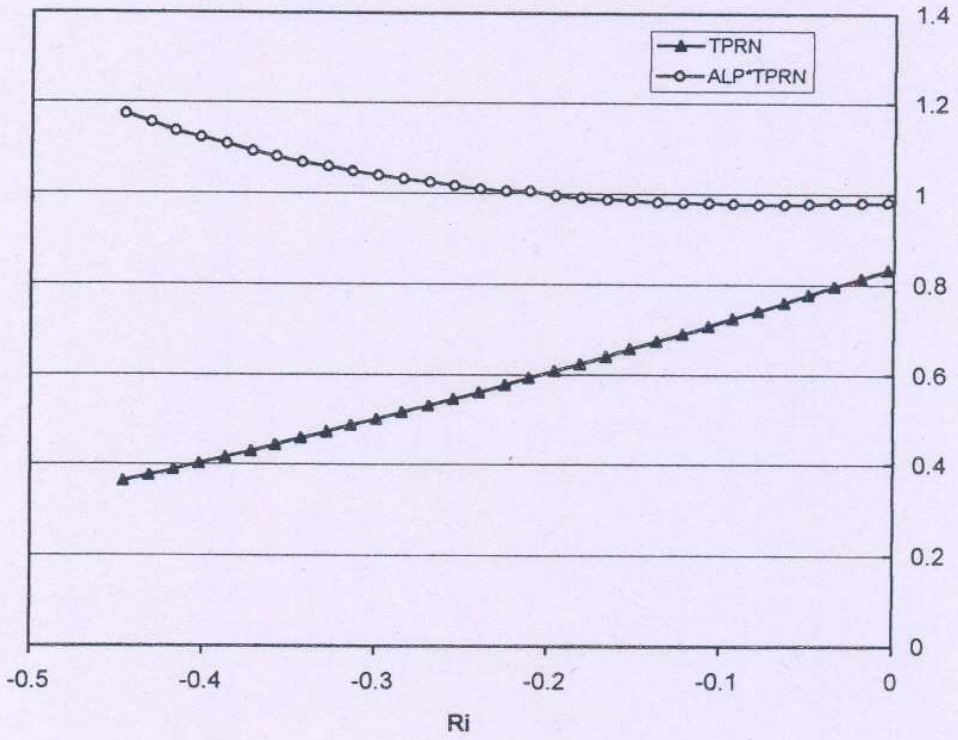

Figure 8(b)

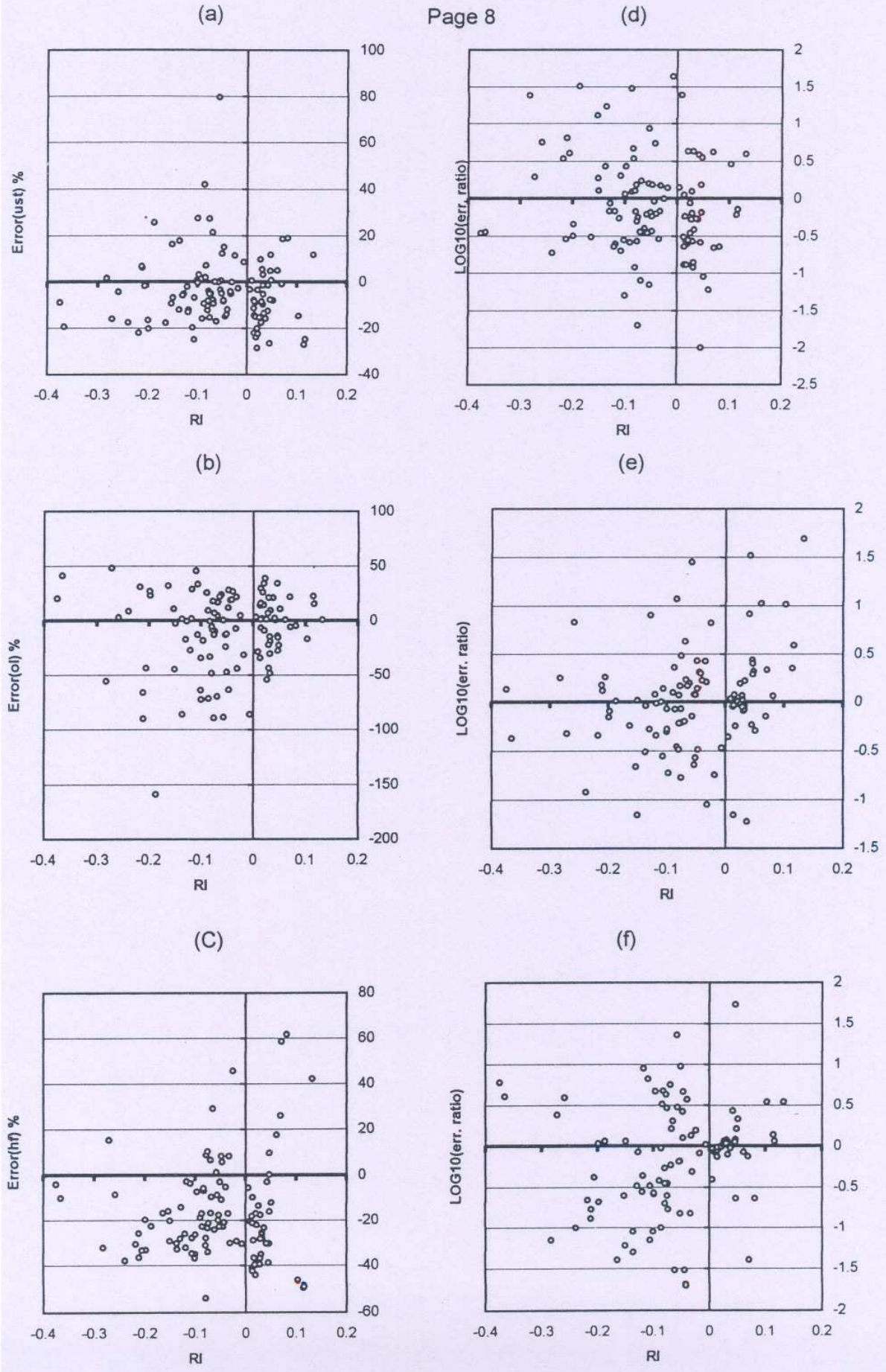
(a)
Error(ust) %
RI
(d)
LOG10(err. ratio)
RI
(b)
Error(oil) %
RI
(e)
LOG10(err. ratio)
RI
(C)
Error(hf) %
RI
(f)
LOG10(err. ratio)
RI

Figure 9

UNSTABLE (SLH/Z > 1)

(a) Wind

(b) Temperature

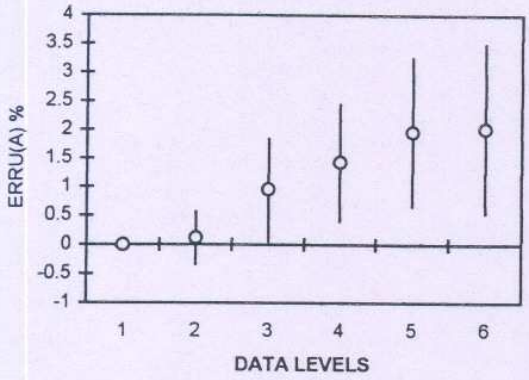

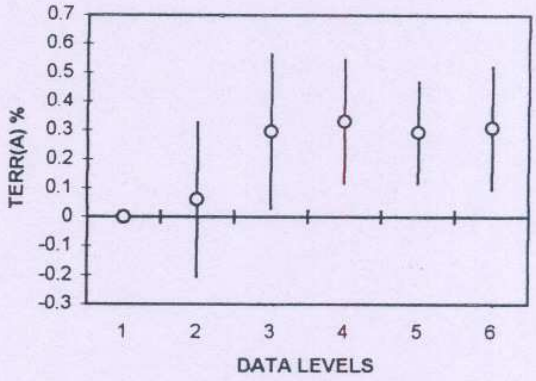

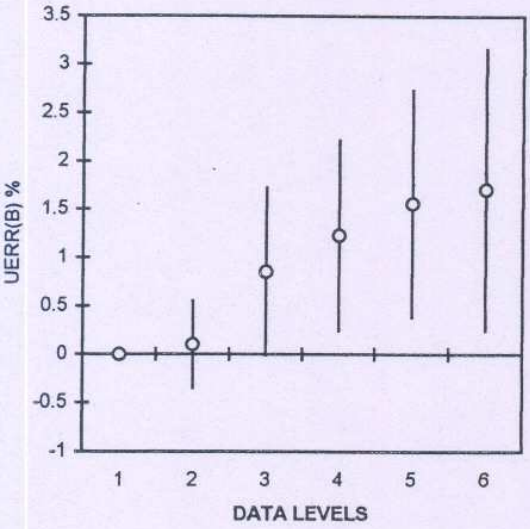

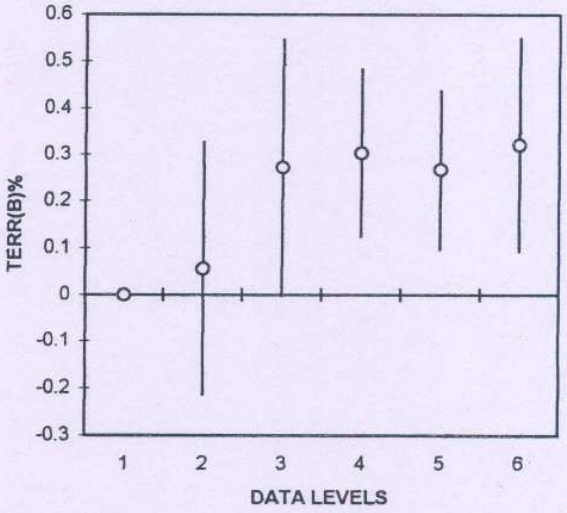

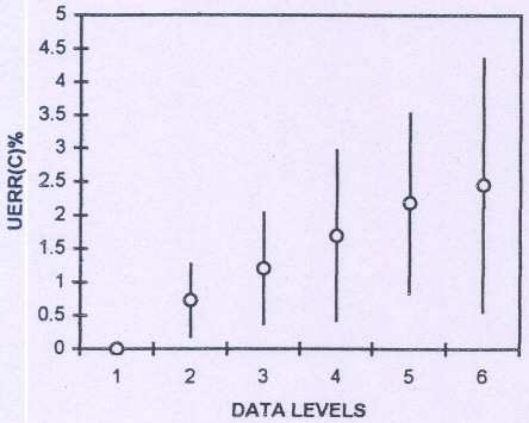

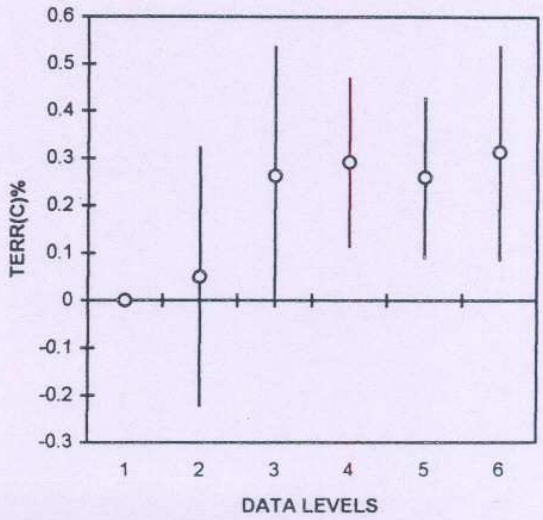

Figure 10

UNSTABLE (SLH/Z < 1)

(a) Wind

(b) Temperature

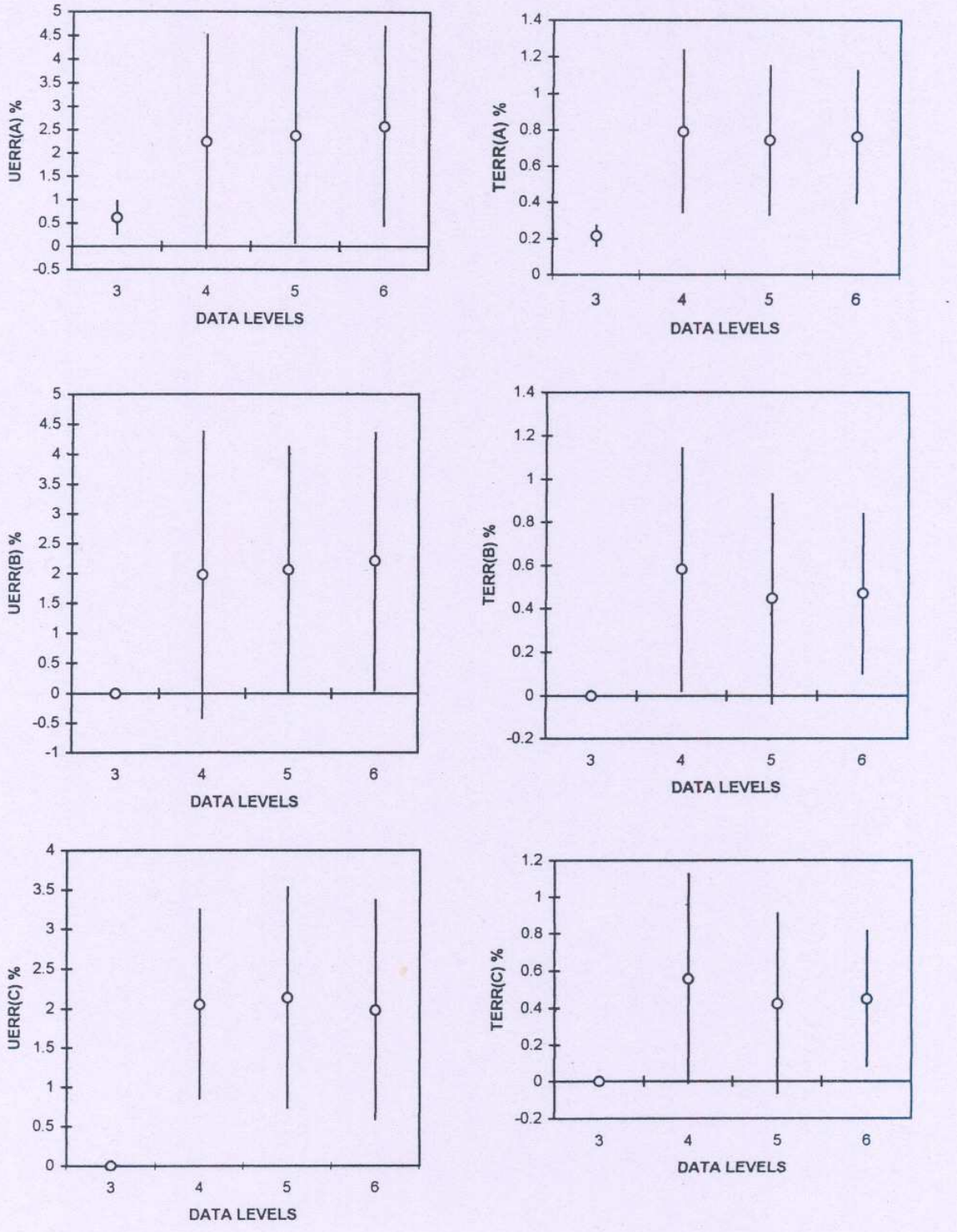

Figure 11

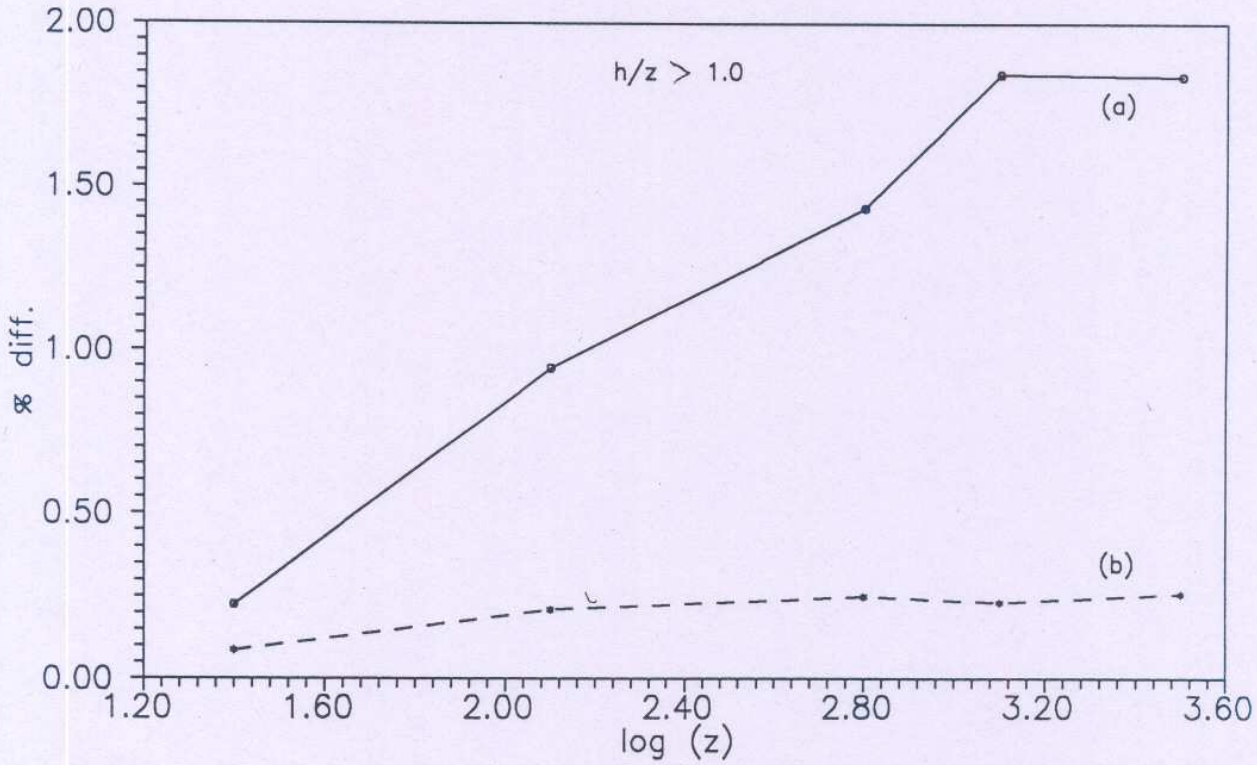
2.00
1.50
1.00
0.50
0.00
% diff.
h/z > 1.0
(a)
(b)
1.20
1.60
2.00
2.40
2.80
3.20
3.60
log (z)

Fig. (12a)

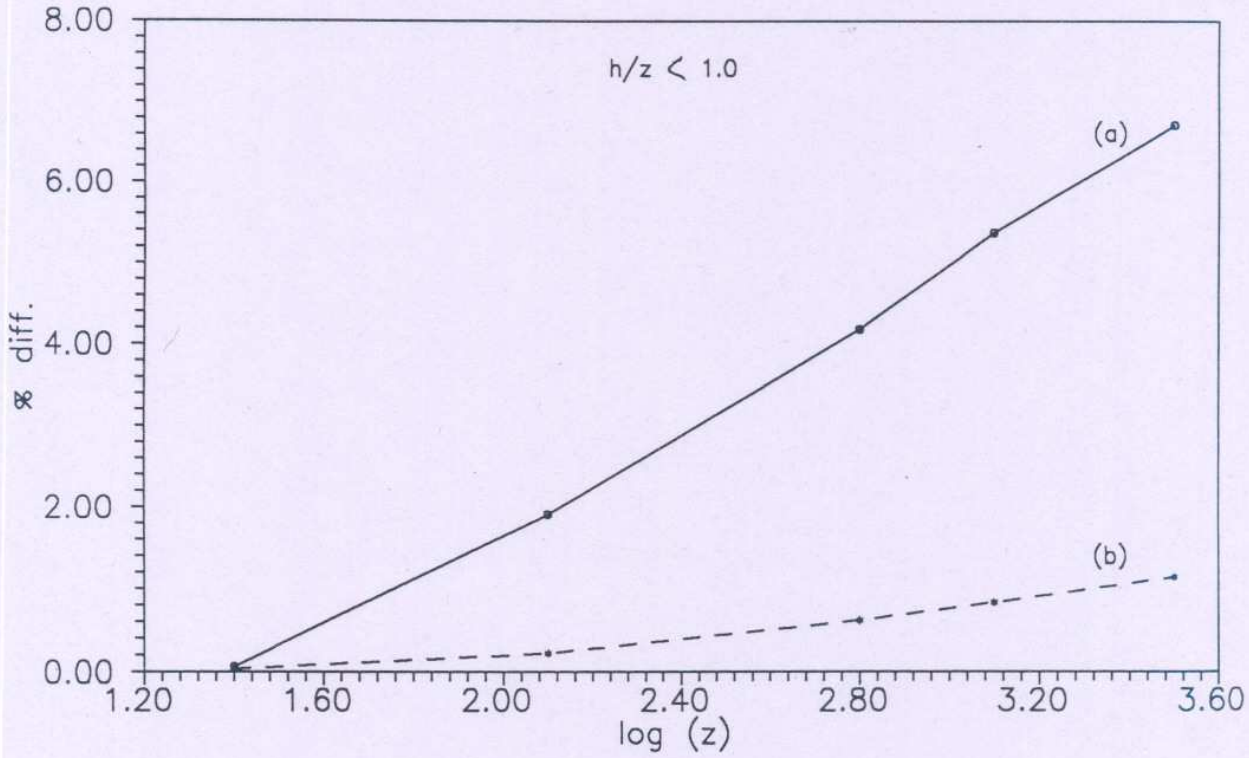
8.00
6.00
4.00
2.00
0.00
% diff.
h/z < 1.0
(a)
(b)
1.20
1.60
2.00
2.40
2.80
3.20
3.60
log (z)

Fig. (12b)

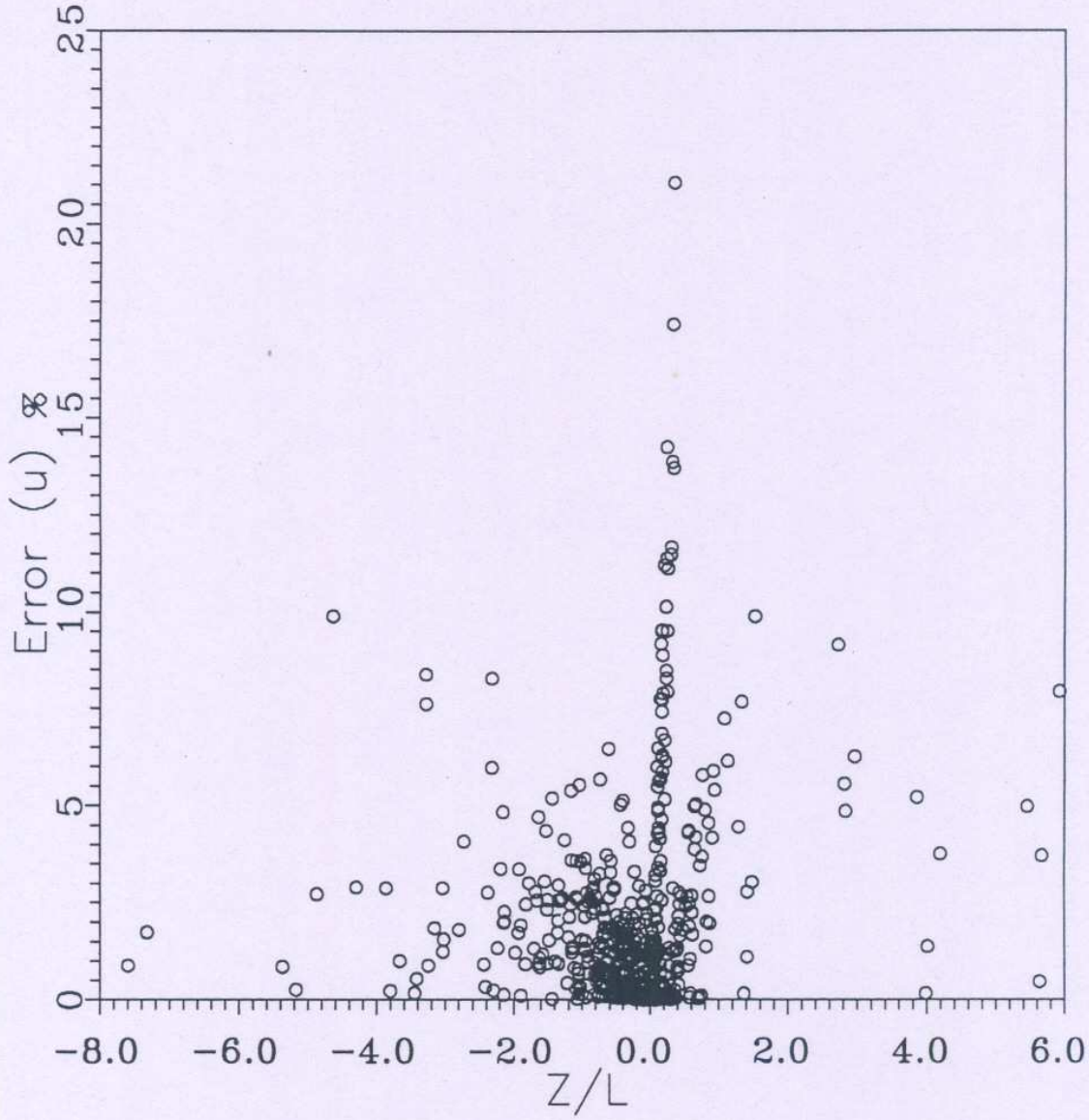

Fig. (13a)

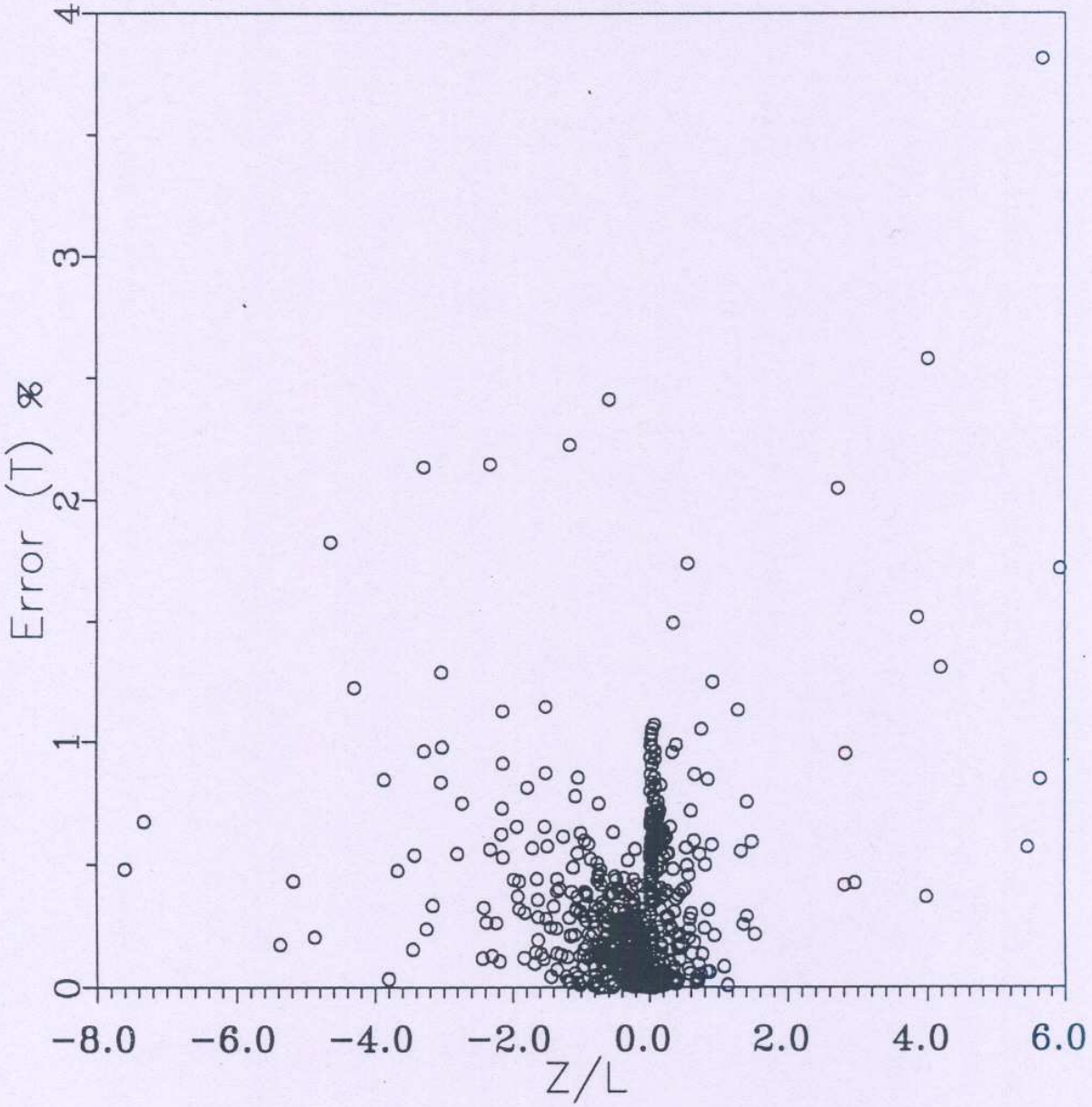

Fig. (13b)